IEEE Access
Multidisciplinary | Rapid Review | Open Access Journal

Received 10 June 2022, accepted 12 August 2022, date of publication 19 August 2022, date of current version 31 August 2022.

Digital Object Identifier 10.1109/ACCESS.2022.3200336

RESEARCH ARTICLE

Optimized Distributive Cross-Layer and Thermal-Aware Convergecast Protocol for Wireless Body Area Network

YASIR SHAHZAD[1], HUMA JAVED[1], HALEEM FARMAN[2], ZAHID KHAN[3], (Senior Member, IEEE), MOUSTAFA M. NASRALLA[4], (Senior Member, IEEE), AND ANIS KOUBAA[3]

[1]Department of Computer Science, University of Peshawar, Peshawar 25120, Pakistan
[2]Department of Computer Science, Islamia College University Peshawar, Peshawar 25120, Pakistan
[3]Robotics and IoT Laboratory, Prince Sultan University, Riyadh 66833, Saudi Arabia
[4]Smart Systems Engineering Laboratory, Department of Communications and Networks Engineering, Prince Sultan University, Riyadh 66833, Saudi Arabia

Corresponding author: Haleem Farman (haleem.farman@icp.edu.pk)

This work was supported by the Robotics and Internet-of-Things Laboratory, Prince Sultan University, Riyadh, Saudi Arabia.

ABSTRACT The Internet of Healthcare Things has significantly altered traditional patient-doctor relationships by allowing essential healthcare treatment from the comfort of one's home. The wireless body area network is an IEEE 802.15.6 standard that focuses on healthcare data, necessitating various cross-layer and thermal-aware protocols. However, most cross-layer protocols have long convergence delays and a single failure point. Moreover, these protocols exploit excessive broadcasts and handshake acknowledgments, causing communication and processing overheads. Furthermore, thermal-aware protocols focus on thermal variations, disperse data collection, and do not support cross-layer techniques. To address these limitations, this study proposes an optimal distributive cross-layer and thermal-aware convergecast protocol. The proposed protocol enforces a novel hybrid convergecast using probability and both minimum attenuation strategies to collect data from leaf nodes to the root to improve data flow and adaptability in the network. In addition, it accelerates the convergence process by reducing recurrent broadcasts and unnecessary acknowledgments, resulting in improved energy efficiency and thermal control. The proposed protocol supports a distributive hierarchy by establishing multiple parent-child relationships to avoid a single root point failure. A multi-parameter maximum benefit-cost function is used to calculate the next hop according to the extracted weights. Packet loss probability validates the number and sequence of packets received at the sink node. The simulation results demonstrate that cross-layer and thermal-aware protocols can coexist effectively. The proposed protocol reduces delays to 19.4%, improves throughput from 8% to 13.75%, and retains a packet loss probability of 0.3% by keeping the thermal rise within bounds.

INDEX TERMS Convergecast, cross-layer, Internet of Healthcare Things, Internet-of-Things, thermal-aware, wireless body area network.

I. INTRODUCTION

The Internet-of-Things (IoT) is the most recent cutting-edge technology that has taken over the technological gamut for tremendous applications in almost all parts of life.

The associate editor coordinating the review of this manuscript and approving it for publication was Taehong Kim.

The IoT vision extends traditional compute-based centralized systems to a dispersed environment by providing a seamless platform for connecting people and objects. It provides a wide range of everyday smart applications in industries [1], education [2], homes [3], cities [4], agriculture [5], and health [6]. The health sector is the most important, with ever-increasing demands providing greater insight into the various platforms for conducting advanced research in this dynamic domain. The traditional patient-doctor physical appointment has lost effectiveness, which upsurges the importance of smart health applications. Smart devices and humans are linked via the Internet for healthcare applications, as shown in Fig. 1.

FIGURE 1. The IoT-based smart rehabilitation system including IoHT.

Essential healthcare, which includes disease prevention, treatment, rehabilitation, and palliative care, is a basic human need for a fit-for-purpose workforce [7]. After a decade of sensor technology research, a wireless body area network (WBAN) is now capable of providing seamless health monitoring of a patient without interfering with his or her normal daily life activities. The WBAN is a specialized application and a subset of a Wireless Sensor Network (WSN). It performs many services as WSN, such as sensing, processing, storing, and communicating within its specified domain. However, WBAN has distinct characteristics where WSN techniques cannot be applied, as shown in Table 1.

TABLE 1. Feature comparison between WSN and WBAN.

Feature	WSN	WBAN
Standard	IEEE 802.15.4	IEEE 802.15.6
Usage	Environment monitoring	Body monitoring
Number of Nodes	Many in hundreds	Few in tens
Node size	Preferably small	Essentially small
Node task	Dedicated	Multiple
Node life	Long in years	Short in months
Node energy	Limited, replaceable	Limited, not replaceable
Data rate	Homogenous	Heterogeneous
Node placement	Dispersed	Congested
Node replacement	Possible	Invasive – not possible
Compatibility	Not necessary	Biocompatible
Topology	Dynamic	Robust
Safety	Less	High
Energy picking	Solar, wind	Vibration, body temperature
Data loss	Tolerated	Prohibited

Data transmission is critical in WBAN, where protocol layers are influenced by a number of factors. The physical layer faces temperature rise, body posture, interoperability, changing topology, interference, battery, and security problems [8]. MAC layer protocols face control packet overhead, broadcasts, convergecast, reliability, delay, collision, and energy problems [9]. The network layer faces routing, localization, mobility, and traffic control problems [10]. The routing protocols in WBAN, such as cross-layer and thermal aware protocols, rely on the conventional three-way handshake convergence process. The convergence process exploits redundant broadcasts and acknowledgments at a cost of high delay. These excessive control packets in the form of acknowledgments during parent-child polling are communication and processing overhead that may also raise the temperature of the sensor nodes, causing adverse effects on body tissues. A single parent is usually selected as a root node, with the others as child nodes. The root node is responsible for collecting all traffic from underlying children and forwarding it to the sink node. The root is a single point of contact having no alternative route, thus failure of this route means failure of the network. Moreover, a broadcast is the only mode of communication between sensors besides their valid entries in the routing table. Another factor that contributes to delays and thermal rise is that packets traveling longer routes require other nodes to do more processing by forwarding data. To address the limitations mentioned above, an optimized distributive cross-layer and thermal-aware routing protocol that can operate adaptively, efficiently, and reliably is required.

This paper proposes a novel cross-layer and thermal-aware routing protocol using an optimized convergecast strategy for a distributive network. The proposed protocol employs a hybrid strategy comprised of gossip-based and attenuation-based convergecast strategies. A gossip-based strategy such as probability convergecast (*ProbaCvg*), increases the probability that a message will reach its destination. Whereas, an attenuation-based strategy such as both minimum attenuation (*BothMinAtt*), aids in providing an alternate route to complete transmission if the primary route fails. Furthermore, the proposed protocols reduce redundant broadcasts during the initialization process, parent-child polling, and convergecast. In addition, acknowledgments are also restricted during parent-child polling. The proposed method also avoids root point failure using a distributive cross-layer approach by enforcing multiple parent-child relationships within two hops.

The convergecast proficiently collects data in many-to-one order using the ProbaCvg strategy, supplemented by a backup BothMinAtt strategy to improve overall data flow and adaptability in the network. The proposed protocol reduces communication and processing overheads while maintaining thermal effects and energy efficiency. Moreover, the sink node verifies the sequence and number of received packets using packet loss probability to ensure accurate data. The research presented in this paper focuses on the best and most optimized path selection parameters such as energy, thermal effect, path loss, link reliability, hop counts, and bandwidth.

The rest of the paper is organized as follows. Section II gives a comprehensive literature review and its associated research limitations. Section III provides the methodology of the proposed protocol. Section IV provides results and discussions, and Section V gives concluding remarks with future directions.

II. LITERATURE REVIEW

The WBAN is a special-purpose network of heterogeneous nodes with cross-layer, temperature-aware, posture-based, cluster-based, and Quality of Service (QoS) based routing classifications [11], as shown in Fig. 2.

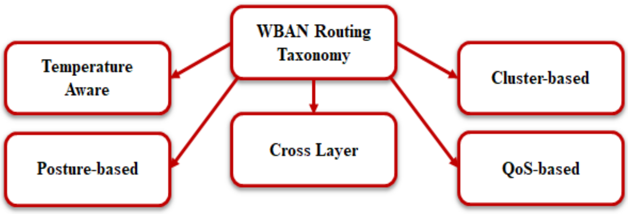

FIGURE 2. Classification of WBAN routing protocols.

A. CROSS-LAYER ROUTING

Cross-layer routing protocols coordinate information from layer to layer by improving synchronization between each other without interfering with the main functionality [12]. Cross-Layer Design Optimal (CLDO) is proposed by [13] to improve transmission reliability, energy efficiency, and network lifetime by working across physical, MAC, and network layers. The protocol seeks optimal transmission power, relay node, and packet size. Joint transmission power control and relay cooperation Autocorrelation-based Adaptive Transmission (ATT) [14] uses the IEEE 802.15.6 standard. Two-hop cooperative transmission, dynamic slot scheduling, and joint transmission power control are used to realize a trade-off between reliable transmission and energy. The scheme predicts channel condition, regulation of transmission power with reordering slot sequence, and relay node selection. Link Reliability and Performance Optimization (LRPO) in WBAN is proposed by [15] to offer a cross-layer routing mechanism using QoS to find a cost function of energy levels of nodes, reliable link availability, and variating specific absorption rates. The algorithm is implemented in two stages, energy efficiency is combined with link reliability policy and QoS contention windows to analyze network performance. The protocol is relay cooperative, where the source node broadcasts route requests to neighbors, who respond with authentic routes.

A Cross-Layer Protocol PHY/MAC (CLPM) for body path loss in the IEEE 802.11ah IoT networks is proposed by [16]. The protocol focuses on retransmissions by nodes that have not received acknowledgment requests. Repetitive requests result in higher communication costs and a higher packet error rate. It detects human body interference via beacon messages and beacon information in order to make transmission decisions. A Priority-Based Cross-Layer Routing Protocol (PCLRP) [17] works across MAC and network layers. The data is prioritized into three categories: *P1* for emergency data, *P2* for time-sensitive data, and *P3* for general data. The protocol provides two competition access phases for child nodes, each of which is further divided into three priority-based slots. Cross-layer Opportunistic MAC/Routing (COMR) for reliable communication on the Internet of health things is proposed by [18]. The protocol offers a cross-layer routing mechanism using QoS to find a cost function of energy levels of nodes, reliable link availability and variating specific absorption rates. The algorithm is implemented in two stages, where energy efficiency is combined with link reliability policy and QoS contention windows to analyze network performance. The source node broadcasts route requests to neighbors, who respond with authentic routes in relay cooperative mode [19].

The above-mentioned protocols use traditional three-way handshakes and recurrent broadcasts for network initialization and data dissemination, imposing additional traffic on children and parent nodes. *Hello* packets are sent at regular intervals with frequent searches for relay nodes. Prediction of channel conditions invites overhead, resulting in massive power feeding, delays, and slow convergence, causing root nodes to run out of energy quickly. Furthermore, the existing protocols are incapable of ensuring reliable transmission of low-priority data because the number of transmitted packets is not validated at the sink node. Below, Table 2 provides an overview of cross-layer protocols.

TABLE 2. Comparison of cross-layer protocols.

Name of Protocol	Delay	Throughput	Reliability	Convergence	Broadcast
PCLRP, 2016	High	Med.	Med.	Med.	High
CLDO, 2017	Med.	High	High	Med.	Med.
ATT, 2018	Med.	High	High	High	Med.
LRPO, 2019	Low	High	High	Med.	High
CLPM, 2020	High	Med.	High	Low	High
COMR, 2021	Low	High	Med.	Med.	High

B. THERMAL-AWARE ROUTING

The wireless modules generate magnetic and electronic radio signals that emit radiation, and exposure to this radiation can directly raise the temperature of sensor nodes and human body tissues. As a result, thermal-aware routing protocols are being developed to mitigate the effects and frequency of hotspots (heated nodes). M-ATTEMPT [20] is a power-proficient and temperature-aware routing protocol that also reduces the lag between heterogeneous bio-medical sensors. The sink node serves as a base station and is located in the body's center, whereas the rest are located in inferior positions. The protocol complies with four stages, such as initialization, routing, organization, and information transmission. Trust and Thermal Aware Routing Protocol (TTRP) [21] considers two parameters, such as temperature and trusted communication via relay nodes. The relay nodes do not participate in information collection and are equipped with high energy to complete tasks. The TTRP protocol includes three stages; trust estimation, route discovery, and a route maintenance stage. A Thermal Aware and Energy Optimized (TAEO) routing protocol for WBAN is proposed by [22]. It addresses the problem of temperature-raised hotspots while improving network stability and lifetime. In the initialization phase, they broadcast their location, energy level, temperature, and node-ID for routing decisions.

High Throughput and Thermal Aware Routing protocol (HTTRP) [23] maintains temperature within specified limits while balancing energy consumption. The forwarding node uses an objective function based on residual energy and node temperature to select the next relay node. The traditional initialization finds neighbors based on parametric values such as neighbor identity, residual energy, and temperature. A thermal-aware duty cycle MAC protocol for IoT healthcare (ThMAC) is proposed by [24] to estimate the tissue temperature in order to maintain adequate thermal levels and avoid hotspots. The protocol achieves QoS by allocating disjoint periods for different types of traffic through the use of a superframe structure. A thermal wake-up schedule specifies the maximum and minimum amount of communication for a given time. A Mobile Temperature Heterogeneity Energy (mobTHE) routing protocol is proposed by [25] to address the disconnection problem during information exchange. Dual coordinator nodes are used to balance trade-offs for efficient synchronization between themselves to minimize packet transmission redundancy and packet drops.

However, the discussed protocols only use temperature as a routing parameter and have a long delay to reduce the occurrence of hotspots. Path selection suffers from additional trade-offs, processing, and transmission complexities. The majority of thermal-aware protocols are non-distributive, broadcast-oriented, energy-hungry, and have low data reliability. Table 3 provides a summarized review of common parameters used in the above-discussed thermal-aware protocols. The comparison criteria are set to low ($0 \approx 30$), medium ($31 \approx 70$), and high ($71 \approx 100$).

TABLE 3. Comparison of thermal-aware protocols.

Name of Protocol	Delay	Throughput	Reliability	PDR	Convergence	Broadcast
M-ATTEMPT, 2013	Low	Med.	Med.	Med.	Med.	Med.
TTRP, 2017	Med.	High	High	High	Med.	Med.
TAEO-A, 2019	High	Low	Low	Low	Low	High
HTTRP, 2020	High	Med.	High	High	High	Low
ThMAC, 2020	Med.	High	Med.	Med.	Med.	Med.
mobTHE, 2021	High	Med.	Med.	Low	Low	High

III. METHODOLOGY

A. RESEARCH BACKGROUND

When WBAN is deployed, it usually starts a route discovery process to find all available nodes and valid links between them. To locate its neighbors, including relay nodes, the parent node broadcasts a route request (R_{REQ}) message. The children confirm their availability by sending a route reply (R_{REP}) message after successfully receiving R_{REQ}. The parent node sends an acknowledgment (Ack) message to the child node to confirm his neighbor's status. All nodes that receive the initial Ack message update their routing tables for the valid path between them. The same process is repeated from the child node by broadcasting the R_{REQ} message on behalf of its parent. The sub-child receiving the message replies with interest to establish valid multihop paths, as shown in Fig. 3.

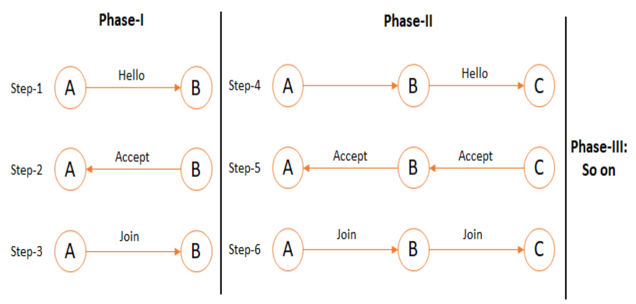

FIGURE 3. Conventional initialization process in WBAN. Root (Node-A) sends *Hello* packet to the child (Node-B). In response, the child sends an *Accept* packet and Node-A responds with a *Join* packet by updating its routing table. The process continues by Node-B towards sub-child (Node-C) and so on.

When a node receives a duplicate R_{REQ}, it avoids the looping paths by comparing the R_{REQ} identifiers. If a node desires to leave, it sends a route leave L_{REQ} message. In the preceding scenario, a single parent begins the convergence process by taking a maximum number of children and also enforcing L_{REQ} message to truncate a child node. The parent node is predefined and acts as a single point of contact, indicating a high degree of dependency. The entire network will fail if the parent node fails to respond to a message or becomes depleted. Moreover, broadcasting is the only mode to discover new routes or establish parent-child associations. Recurrent broadcasting, in addition to valid routing table entries, adds additional processing and communication overhead. Typically, the packet will take the shortest available route to complete the communication until it reaches the assigned threshold or time to live. When a running job is interrupted, data packets wait for the next parent-child election, which compromises data, particularly in emergency communications. The entire procedure is depicted in Fig. 4.

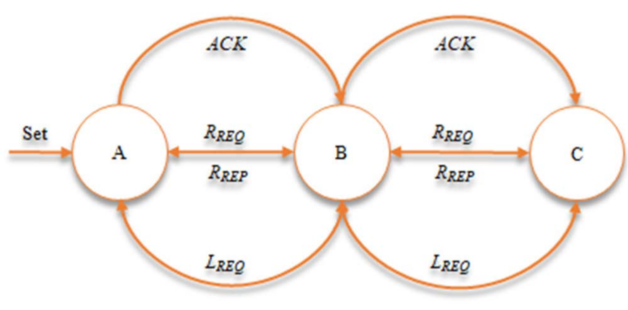

FIGURE 4. Conventional initialization process between Node-A (root), Node-B (child), and Node-C (sub-child).

B. PROPOSED INITIALIZATION

The proposed routing protocol addresses the aforementioned limitations by initiating restrained convergence to gain rapid stability, distributive parent-child relationships to avoid a single root point failure, and an optimized convergecast mechanism for efficient, reliable, and adaptable data flow by maintaining minimal thermal variations.

The proposed protocol improves the initialization process by reducing recurrent broadcasts and excessive handshake acknowledgments during parent-child polling. Initially, it allows the conventional convergence process to find nodes and establish valid communication links between them. The proposed protocol adds an additional feature $R_{REQ} - Wait$ and $R_{REP} - Wait$. The wait feature allows nodes to wait for control packets if they are not collected. The root node (i.e., node-A) awaits a reply R_{REP} message from a child node (i.e., node-B and C), whereas the child node awaits R_{REQ} offers from the root node. When the wait timer runs out, the child node broadcasts its self-availability to join the network. If they remain unanswered in either case, the node begins the initialization process, as shown in Fig. 5.

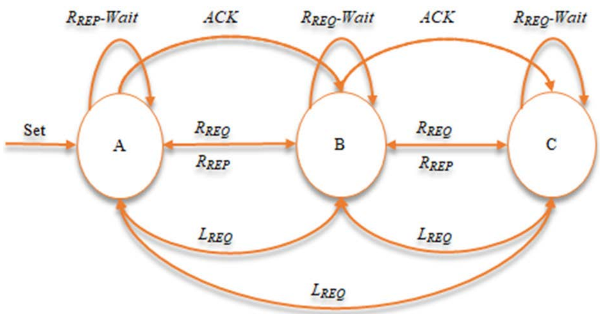

FIGURE 5. Proposed initialization process.

Moreover, if a node has routing table entries, R_{REP} is inadmissible in the subsequent discovery phase because the previous information is already available in the routing table. The overall process is illustrated in Table 4.

The calculated complexity during the initialization process is primarily determined by the amount of time and space required for broadcast communication initiated by the parent node. The initialization process has a time complexity of $O(V)$, where v is the number of nodes. Whereas, space complexity is $O(mV)$, where m is the memory requirement for each child that depends on a size of a single broadcast packet. All other communication has a constant time and space complexity of $o(1)$ for $o(v)$.

C. PROPOSED NETWORK MODEL

WBAN is made up of tiny sensors that are either invasive or non-invasive biosensors powered by micro-batteries and are responsible for sensing physiological data. The sensed data is gathered, cleaned, and transformed into a useful shape to predict the health status of a patient [26]. The WBAN architecture supports three kinds of data transmission, such as normal, on-demand, and emergency data. Emergency data is more sensitive, requiring high priority P_H for early processing. On-demand transmission P_D is a user-enquired request that is also treated for early processing and execution, similar to P_H. On the other hand, normal data P_N is periodic and continuous traffic towards the sink. Graceful degradation is performed by nodes with low energy by sending E_{LOW} messages to stop forwarding packets, whereas thermal effects are flagged by sending T_{HIGH} messages. These messages are sent as an alarm for low energy and high temperature to inform neighbors to refrain from sending data. Both messages initiate a waiting process to gain energy or cool down. However, WBAN is a critical network and if a node has P_H packets then it must complete ongoing transmission and then go to sleep immediately. In the referred situation, the proposed convergecast initiate BothMinAtt strategy to take over ProbaCvg. The proposed protocol also ensures that a route is not re-engaged for a second transmission in order to give other nodes an equal opportunity to act as a forwarding node.

TABLE 4. Pseudocode of initialization process and parent-child polling.

Pseudocode – Initialization( )
Deploy Purposeful Sensors
 # Finding nodes
 # Establishing a stable communication link
If (node is ready)
Parent → Broadcast R_{REQ}
Children → Reply R_{REP}
Parent → Send Ack && create routing table
Children → Compute parameters (initial energy, temperature, attenuation, hop count, link status) && create routing table && update entries && share parameters
Else
Parent → $R_{REP} - Wait$ && Broadcast R_{REQ}
Children → $R_{REQ} - Wait$ && Broadcast R_{REP}
End
 # Network is converged
 # Parent child polling without acknowledgment
Repeat
If (hop_count ≤ 2 && routing table is updated)
Parent → Multicast offer
Children → Unicast Consent
Else (call initialization process)
Until (maximum relationships within two hops)

WBAN is a critical network on which human life depends. As a result, data priority is essential for determining the packet priority to reach the base station, especially in emergencies. The proposed model in this research prioritizes the values under the MAC layer contention window ($CWin$) in order to define the standard based on data classes. The maximum and minimum values are assigned to differentiate the traffic according to its type, ranging from background traffic to the most critical emergency traffic. The proposed model efficiently differentiates traffic to allow appropriate transmission for P_N and P_H. There are several priority levels and contention windows available in the literature [27]. However, due to limited resources, a simple three-tiered data priority system is proposed for P_N, P_D, and P_H communication, as given in Table-5. The complete block diagram of the proposed model is illustrated in Fig. 6.

TABLE 5. Assigned priority to data packets.

Traffic Type	Priority	CtWnMin	CtWnMax
Emergency	P_H – High	1	8
On-demand	P_D – Medium	8	32
Normal	P_N – Low	16	64

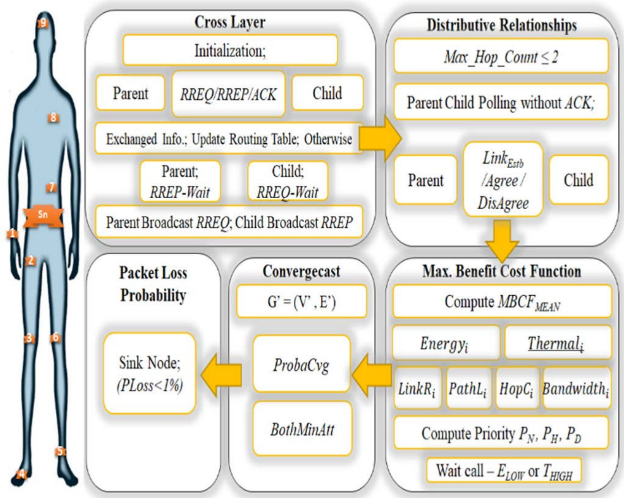

FIGURE 6. Block diagram.

1) ENERGY MODEL

Energy is a front-line parameter in all resource-constraint networks because it is critical to the network lifetime [28]. WBAN, a resource-constraint network, suffers from energy-hungry inter-WBAN or intra-WBAN communications, especially in broadcasts and multicasts, because it needs more transmission power than unicast [29]. Periodic sensing consumes 10% more energy in comparison to emergency and on-demand communication, whereas relay nodes consume 20% more energy than standard nodes [30]. The total energy (E_{TOT}) consumed by a standard node (SN) is the sum of sensing activity, radio transmission and reception, internal processing, and thermal rise given in (1).

$$E_{TOT\rightarrow SN} = E_{SENSE\rightarrow SN} + E_{TRANS/RECEP\rightarrow SN} + E_{PROCESS\rightarrow SN} + E_{THERMAL\rightarrow SN} \quad (1)$$

whereas the total energy consumed by a relay node (RN) is given in (2).

$$E_{TOT\rightarrow RN} = E_{SENSE\rightarrow RN} + E_{TRANS/RECEP\rightarrow RN} + E_{PROCESS\rightarrow RN} + E_{THERMAL\rightarrow RN} \quad (2)$$

2) THERMAL EFFECT MODEL

The thermal effect, an important parameter in WBAN, is the increase in temperature of a sensor node. The sensor nodes heat up due to steady processing and communication. These sensors are installed invasively or noninvasively on the human body, having a significant impact on the underlying tissues, which may be damaged by thermal rise. In the above-discussed literature, when thermal-aware protocols detect hotspots, it results in unnecessary delays, causing a negative impact on data communication and resulting in decreased network stability and lifetime. The proposed protocol adaptively handles the stated situation by considering thermal rise along with other necessary metrics. If a hotspot is detected, the data is routed to the next best path using the BothMinAtt convergecast strategy, as illustrated in Fig. 7.

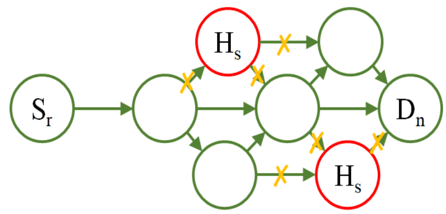

FIGURE 7. *Sr* desire to send a packet to *Dn* will not be routed to/from *Hs*.

There are two types of thermal effects, such as heat generated by nodes and heat influenced by tissues, the latter of which is highly dependent on the former. The expected rise in thermal effect (RTE_{EXP}) can be estimated in (3).

$$RTE_{EXP} = TN_{PACKET} \times Avg \times TR_{PACKET} \quad (3)$$

where TN_{PACKET} is the total number of packets, the average temperature (Avg), and TR_{PACKET} is the temperature rise. From (3), the total thermal effect (TTE) of the node can be calculated by adding the current node temperature (CT_{NODE}) and RTE_{EXP} as computed below in (4).

$$TTE = CT_{NODE} + RTE_{EXP} \quad (4)$$

Specific Absorption Rate (SAR) is an important technique for calculating the amount of radiation absorbed by body tissues, which is useful for determining the heat absorption rate per unit mass [31]. WBAN typically performs in congested environments, where it constantly forwards vital data despite congestion, disconnected links, and delays. Continuous requests for successful transmission are made via electromagnetic radiation, which results in radiated thermal energy. As the sensors are installed invasively or non-invasively on the human body, exceeding radiation limits is extremely harmful to body tissues, necessitating the use of SAR techniques to reduce the biological risks. The radiation of a sensor node during packet transmission is directly proportional to its power and the distance between nodes. As the distance between sensor nodes increases, so does the SAR level, which necessitates more power and raising the temperature of the nodes. The SAR is heat produced on tissue conductivity (σ)

by the induced electromagnetic field radiation (EMF) and the density of tissue (ρ) can be estimated in (5).

$$SAR = \frac{\sigma(EMF)^2}{\rho} \quad (5)$$

Keeping in view above, the total change in thermal effect (ΔT) beneath the tissue of the sensor node is equal to SAR in the time interval (t) overheat capacity (c) given in (6).

$$\Delta T = (SAR)\,\frac{t}{c} \quad (6)$$

3) LINK RELIABILITY AND PATH LOSS MODEL

Estimating packet drop rate is an important parameter for a reliable network. Typically, the link reliability (LR) between node x and y can be determined by successful packet transmission (PT_S) over total packet transmission (PT_{TOT}) for an average weight factor (η) between xy [32] is given in (7).

$$LR_{xy} = (1-\eta)\,LR_{xy} + \eta\frac{PT_{S\rightarrow xy}}{PT_{TOT\rightarrow xy}} \quad (7)$$

The transmitted signals attenuate as a result of travel, clothing, implants, and body postures. The proposed protocol describes a path loss between nodes for temporal variation of body path loss propagation. To relate path loss to the total distance (d), frequency (f) as per the standard loss equation of Friis free space, path loss (PL) between two communicating nodes in consumed distance d_0 adding the path loss exponent (p) [32] is computed in (8).

$$PL_{d.f} = PLoss_{d_0} + 10p.log_{10}\left(\frac{d}{d_0}\right) \quad (8)$$

where

$$PL_{d_0} = 10.\log_{10}.\frac{(4\pi d_0 f)^2}{c} \quad (9)$$

where f is the actual node frequency and c is the speed of light. In the proposed protocol, packet forwarding causes variations that necessitate a shadowing factor to rectify the path loss deviation from its mean value. Therefore, a Gaussian distributed shadowing factor (X_σ) is added with a zero mean and standard deviation (σ) for the path loss function given in (10).

$$PLoss = PLoss_d + X_\sigma \quad (10)$$

D. MULTI-PARAMETER MAXIMUM BENEFIT COST FUNCTION

A multi-parameter maximum benefit cost function computes the next hop based on the extracted weights, which include residual energy, thermal effect, path loss, and link reliability parameters [33]. The sum with a weighted coefficient is used to find the best next hop with the highest value. As previously stated, energy is the most important and necessary metric to consider when looking for the next best hop. The proposed protocol monitors neighboring node energy levels and selects a route with high residual energy values to provide equal node participation opportunities, resulting in longer network life. If the calculated MBCF value is less than the assigned threshold, the node will not act as a forwarding node but may send emergency data if detected.

Equation (1) calculates the energy level of a node. To declare a threshold of energy level, MBCF ($\gamma_i 1$) is the variance between the total residual energy (RE_{TOT}) and node's initial energy (NE_{INI}) levels with the assigned minimum energy thresholds of the nodes ($E_{MIN.TH}$) is given in (11).

$$\gamma_i 1 = \frac{RE_{TOT} - E_{MIN.TH}}{NE_{INI} - E_{MIN.TH}} \quad (11)$$

Equation (6) computes the thermal variations of a node. To declare a threshold of node temperature, the MBCF ($\gamma_i 2$) is the difference between the total thermal effect of a node (ΔT_N) and the initial thermal value of a node ($\Delta T_{N.INI}$) levels with assigned minimum thresholds (ΔT_{MIN}) is given in (12).

$$\gamma_i 2 = \frac{\Delta T_N - \Delta T_{MIN}}{\Delta T_{N.INI} - \Delta T_{MIN}} \quad (12)$$

Equation (7) computes the link reliability between nodes. To declare a threshold of link reliability, the MBCF ($\gamma_i 3$) is the difference between total residual link reliability (LR_{TOT}) and the maximum value of a node (LR_{MAX}) with assigned minimum thresholds of the nodes ($LR_{MIN.TH}$) is given in (13).

$$\gamma_i 3 = \frac{LR_{TOT} - LR_{MIN.TH}}{LR_{MAX} - LR_{MIN.TH}} \quad (13)$$

Equation (10) computes path loss between sensor nodes. To declare a threshold, an MBCF ($\gamma_i 4$) is the difference between total path loss (PL_{TOT}) and maximum path loss of a node (PL_{MAX}) with assigned minimum thresholds of the nodes ($PL_{MIN.TH}$) is given in (14).

$$\gamma_i 4 = \frac{PL_{TOT} - PL_{MIN.TH}}{PL_{MAX} - PL_{MIN.TH}} \quad (14)$$

Hop count ($\gamma_i 5$) and available bandwidth ($\gamma_i 6$) are taken into account to strengthen the next best hop selection criterion. These parameters ensure more reliable data transmission, improve network performance, reduce transmission delay and improve node-to-node communication in real-time. The HC depends on candidate hops to the sink (HC_{NEXT}) over the total hops of candidate nodes towards the sink node (HC_{TOT}) is estimated in (15).

$$\gamma_i 5 = \frac{HC_{NEXT}}{HC_{TOT}} \quad (15)$$

The $\gamma_i 6$ is the difference between accessible bandwidth (BW_{AC}) and total bandwidth (BW_{MAX}) with an assigned minimum threshold (BW_{MIN}) given in (16).

$$\gamma_i 6 = \frac{BW_{AC} - BW_{MIN}}{BW_{MAX} - BW_{MIN}} \quad (16)$$

The above-estimated parameters are linearly summed to conclude MBCF by evaluating parameters for the selection of the next best hop. The mean MBCF is given in (17).

$$MBCF_{MEAN} = \alpha \times \gamma_i 1 + ß \times \gamma_i 2 + \eta \times \gamma_i 3 + \theta \times \gamma_i 4 + \nu \times \gamma_i 5 + \lambda \times (1 - \gamma_i 6) \quad (17)$$

Here α, ß, η, θ, ν, λ are weight factors of each parameter, and $\sum_{i=1}^{n}(\alpha + ß + \eta + \theta + \nu + \lambda) = 1$. In order to obtain the maximum value from the above equation, an argument *Argmax* operation is computed in (18).

$$\begin{aligned}\hat{\imath} &= \text{argmax}\{\text{MBCF}_{MEAN}\}\\ &= argmax_i\{\alpha \times \gamma_i 1 + ß \times \gamma_i 2\\ &\quad + \eta \times \gamma_i 3 + \theta \times \gamma_i 4 + \nu \times \gamma_i 5 + \lambda \times (1 - \gamma_i 6)\} \end{aligned} \tag{18}$$

where $i = 1, 2, 3, 4, \ldots.., N$

TABLE 6. Pseudocode of MBCF and route truncate.

```
Pseudocode – MBCF and Route Truncate( )
# Computing routing cost
# Assign packet priority
MBCF
Compute γi1 , γi2 , γi3 , γi4 , γi5 , γi6
Compute MBCF_MEAN
  If Priority == P_H && MBCF == highest
        Forward packet to the sink
  Else
        If Priority == P_D | P_N && γi1 | γi2 ≥ threshold OR
          MBCF_MEAN == highest
        Forward packet to the next hop
        End
  End
# Tree or node truncate
Route leave request
  If γi1 ≤ E_MIN.TH
    Do not forward a packet
    Send E_LOW
    Send L_REQ
        If γi2 ≥ ΔT_MAX
          Do not forward a packet
          Send T_HIGH
          Initiate cool-down cycle
          Request alternative route
                If γi3 , γi6,≤ MIN.TH &&
                 γi4 , γi5 > MAX.TH
                 Do not forward a packet
                 Send L_REQ
End If All
Purge route
Repeat
```

The computational complexity of MBCF revolves around parametric computation and its mean value. The process proceeds iteratively for overall time and space complexity $O(P)$ where p is a parametric computation. For the number of nodes V, the complexity becomes $O(VP)$ at a constant time and space of $o(1)$.

E. PACKET LOSS PROBABILITY

The proposed network has successfully converged, and stable communication links are identified for packets to choose the next best hop. The sequence and number of traveling packets that reach the sink node must be confirmed to ensure that the data is accurate. The packet error rate (P^{ER}) is used to calculate the number of packets that arrive in their original form at the sink or base station. The bit error probability (P^{BE}) is a standard technique to calculate the bit difference between the transmission sequence and received bits [34] is given in (19).

$$P^{ER} = 1 - (1 - P^{BE})^{TPL+PHL} \tag{19}$$

where *TPL* is a transmitted packet length and *PHL* is packet header length. Moreover, other factors, such as signal-to-noise ratio (*SNR*), distortion, and jitter, have an impact on the calculated values [35]. The stated conditions must be defined to reduce the error rate by taking into account the source (*SE*), destination (*DN*), and relay (*RY*). The inclusion of relay nodes adds an extra helping hand to enhance network performance and lifetime [36]. These nodes are involved in two-way communication, and there is a chance that an error will occur between *SE* and *DN* or *SE* and *RY* nodes. If the former fails, the latter is error-free, and data is transmitted from *SE* to *RY*, failing *DN* to *RY*, and vice versa. Another possibility is that *SE* to *DN* communication fails; therefore, a link between *SE* and *RY* is required. The adaptable link is established by ensuring that the *DN* to *RY* connection is error-free. If any link from *SE* to *DN*, *SE* to *RY*, or *RY* to *DN* fails, it results in a disastrous state, which is not a characteristic of WBAN. As a result, possible link or packet recovery is a fundamental responsibility of a protocol to achieve two-way successful cooperation between nodes. The complete scenario is computed in (20).

$$\begin{aligned}P^{ER}_{2WAY} &= P^{ER}_{SE\to DN,RY} + P^{ER}_{SE\to DN}\left(1 - P^{ER}_{SE\to RY}\right)\\ &\quad\times P^{ER}_{DN\to RY} + P^{ER}_{SE\to DN}\left(1 - P^{ER}_{SE\to RY}\right)\\ &\quad\times (1 - P^{ER}_{DN\to RY})(1 - P^{ER}_{RY\to SR})P^{ER}_{RY\to DN}\end{aligned} \tag{20}$$

F. END TO END DELAY AND THROUGHPUT

In WBAN, the End-to-End ($E2E$) delay is the total time (T) required to transmit a packet P_{LEN} with defined transmission T_{RATE}. Physical *(PHY)* and *MAC* layer services ought to provide additional services such as *PHY* layer packet preamble, *PHY/MAC* layer headers, control frames, inter-frame spacing, and backoff time. The proposed model modifies the propositions and assumptions depicted in [37]. A contention time window (*CtWin*) for a single packet is defined by the meantime collision TE_{COL}, successful transmission TR_{SUC} and failure time TE_{FAIL} by transmission rate. *E2E* is given in (21).

$$E2E = \frac{P_{LEN}}{T_{RATE}} x\,(TE_{COL} + TR_{SUC} + TE_{FAIL}) \tag{21}$$

Here TE_{COL} is the average contention time that occurs due to collisions, backoff time, data packets, acknowledgment duration, short inter-frame space (*SIFS*), and double delay time (α) is given in (22).

$$TE_{COL} = T_{CWIN} + T_{DATA} + T_{(1-ACK)} + 2T_{pSIFS} + 2T_{\alpha} \tag{22}$$

Here the backoff counter is set to a random integer number that is uniformly distributed over the interval [*1, CtWin*] where $CtWin \in (CtWinMin, CtWinMax)$. The backoff time is equal to the carrier sense multiple access (*CSMA*) slot length in the contention window is given in (23).

$$T_{CWIN} = T_s CWin \tag{23}$$

The time required for data packet transmission is given as the sum of packet preamble time, *PHY/MAC* header time, frame check sequence (*FCS*) time, and *MAC* frame body time is given in (24).

$$T_{DATA} = T_{PREAMBLE} + T_{PHY} + T_{MAC} + T_{FCS} + T_{BODY} \tag{24}$$

The required time for acknowledgment is given in (25).

$$T_{1-ACK} = T_{PREAMBLE} + T_{PHY} + T_{MAC} + T_{FCS} \tag{25}$$

Additionally, the radio frequency (*RF*) activity can also be estimated in (26).

$$T_{ACTIVITY} = T_{RFPowerON} + T_{CWIN} + T_{DATA} + T_{(1-ACK)} + 2T_{pSIFS} + 2T_{\alpha} \tag{26}$$

Average positive transmission is equal to the critical data index (*CDIndex*) of *SE* to *DN* and *RF* time activity ($T^{SE\to DN}_{ACTIVITY}$) is typically $T_{RFPowerON} + T_{CWIN}$. A probability P_O is added for *SE* to *DN* communication link, which should be greater than *SE* to *RE* and RE to *DN* links. TR_{SUC} is given in (27).

$$\begin{aligned} TR_{SUC} = {} & CDIndex \Big(T^{SE\to DN}_{ACTIVITY} \cdot P^{SE}_{SE\to DN} \cdot P^{*}_{O} \\ & + \left(T^{SE\to DN}_{ACTIVITY} + T^{RY\to DN}_{ACTIVITY} \right) \left(1 - P^{SE}_{SE\to DN} \right) \\ & \times \left(1 - P^{*}_{O} \right) \cdot P^{SE}_{SE\to RY} \cdot P^{SE}_{RY\to DN} \Big) \\ & + (1 - CDIndex) \cdot P^{SE}_{SE\to DN} \cdot T^{SE\to DN}_{ACTIVITY} \end{aligned} \tag{27}$$

$$\begin{aligned} TR_{SUC} = {} & CDIndex \left(T^{SE\to DN}_{ACTIVITY} + T^{RY\to DN}_{ACTIVITY} \right) \\ & \times \left(1 - P^{SE}_{SE\to DN} \right) \cdot P^{SE}_{SE\to RY} \cdot P^{SE}_{RY\to DN} \\ & + P^{SE}_{SE\to DN} \cdot T^{SE\to DN}_{ACTIVITY} \end{aligned} \tag{28}$$

CDIndex reaches 1, either $T^{SE\to DN}_{ACTIVITY}$ or $T^{SE\to DN}_{ACTIVITY} + T^{RY\to DN}_{ACTIVITY}$ is the time required to send data. If *CDIndex* reaches 0, then $T^{SE\to DN}_{ACTIVITY}$ is the only time required to send.

Finally, TE_{FAIL} can be given in (29).

$$\begin{aligned} TE_{FAIL} = {} & \left(1 - P^{SE}_{SE\to DN} \right) \left(-P^{SE}_{SE\to RY} \right) \cdot P^{SE}_{RY\to DN} \cdot P^{*}_{O} \\ & \cdot T^{SE\to DN}_{ACTIVITY} + \left(1 - P^{*}_{O} \right) \left(\left(T^{SE\to DN}_{ACTIVITY} + T^{RY\to DN}_{ACTIVITY} \right) \right. \\ & \times \left(1 - P^{SE}_{SE\to DN} \right) \left(1 - P^{SE}_{RY\to DN} \right) \cdot P^{SE}_{SE\to RY} \\ & + \left(1 - P^{SE}_{SE\to DN} \right) \left(1 - P^{SE}_{SE\to RY} \right) \left(1 - P^{SE}_{RY\to DN} \right) \\ & \left. \cdot T^{SE\to DN}_{ACTIVITY} \right) \end{aligned} \tag{29}$$

The first section of TE_{FAIL} endorses the link outages of *SE* to *DN* and *SE* to *RY*, whereas *RY* to *DN* is operational. The second section supports the link outages of *SE* to *DN* and *RY* to *DN*, whereas *SE* to *RY* is now operational. The final section endorses outage events *SE* to *DN*, *SE* to *RY*, and *SE* to *DN*. *CDIndex* is excluded because channel fading is unaffected by data type. Maximum throughput (*MaxThPt*) for the proposed protocol can now be calculated as the number of maximum transmissions sent in unit time for $TR_{SUCCESS}$ is given in (30).

$$MaxThPut = \frac{TR_{MAX} x TR_{SUCCESS}}{E2E} \tag{30}$$

In order to improve throughput, payload length PD_{LEN} is added as an additional parameter given in (31).

$$MaxThPut = \frac{TR_{MAX} x TR_{SUCCESS}}{E2E} (PD_{LEN}) \tag{31}$$

G. CONVERGECAST

Convergecast is many-to-one communication that has an important role in Ad-hoc, WSN, Delay Tolerant Network (DTN), and WBAN networks. WBAN prefers a tree-based packet relay model to achieve a higher degree of reliability, where each node sends data to its parent. The parent node is liable to forward the received data as separate packets to the sink or base station. Convergecast methods create trees in many to one, i.e. for a single receiver to N-source ($1 \times N$), for efficient results, despite the hostile nature of WBAN. There are five convergecast classes supported by the literature, such as tree-based, integer programming, multi-paths, time allocation, and flow-based schemes [38]. This paper proposes an optimized convergecast mechanism based on a novel hybrid strategy that extracts the strengths and weaknesses of existing WBAN convergecast approaches.

1) GOSSIP AND ATTENUATION BASED STRATEGIES

The gossip-based algorithms, such as ProbaCvg, maximize the probability of spreading messages to neighboring nodes to reach the destination. These strategies are mostly used when there is no or little knowledge available about the network. If any node desires to send data, it broadcasts a message and ensures successful communication by flooding a message for a probability $P > 0$. The neighbors received messages with a stated probability until all the packets arrived or the time to live (TTL) is reached. Initially, *P* is set to [1:0] so that a node selects a random variable *r* and compares it to *P*, except for the parent node, which decides whether or not to re-broadcast such that $r < P$. It enables the node to decide whether to transmit the message, otherwise, the message is discarded. The forwarding probability is included in the initial broadcast, and the node divides *P* by 2 after each transmission. The performance is near-optimal with respect to delay, however redundant broadcast and replicating messages are transmission overheads.

On the other hand, attenuation-based strategies collect channel attenuation levels before transmission and decide to forward or to hold a message and also decide to which node it forwards. A node that desires to communicate sends a packet *Att.Request.Ask* for an average attenuation value of neighboring nodes towards the parent. The referred strategy selects the lowest value of replying nodes and forwards the packet to them. The only stipulation is that if no response is received after a *wait_time*, the retransmission request is sent. BothMinAtt supports dual node adoption, which can be used to provide backup route adaptability.

2) PROPOSED CONVERGECAST MODEL

To model an optimized convergecast, consider an undirected graph $G = (V, E)$, where $V = (S_0, S_1, S_2, \ldots, S_n)$ represents the set of vertices of sensor nodes and $E = \{(S_a, S_b)\}d(S_a, S_b) \le L$, where $S_a, S_b \in V\}$ represents the set of edges of wireless links between $V(G)$ and L is the length between sensor nodes. Assume that $C_T = (V, E')$ is a convergecast tree graph G with the fewest hop counts $H_{a,b} \le 2$ and within communication range from all the vertices towards the root node, where $E' \subset E$. Consider the root node of the sequence to be S_0. For a given node S_a, assume that P_a is the parent node and Q_a is the direct child of node S_0 in C_T. Additionally, given two nodes S_a and S_b, assume $H_{a,b}$ is the hop count from a to b.

The convergecast is concerned with raw data generated at a constant rate of D in unit time T. The D is generated as shown in (18), (21), and (31). The sensed data is routed towards the root S_0 in delivery time T. Collision detection is requested at this step [39] to refrain from retransmission in order to reduce T. Such that node S_a and all neighbor nodes s_b with a hop count $H_{a,b} \le 2$ refrain from the transmission [40]. So, the final optimized convergecast tree is $G' = (V', E')$ where V', is a set of sensor nodes including the sink node and E' are valid communication links.

As previously stated, ProbaCvg broadcasts a message to flood all of its neighbors. The process is optimized by reducing recurrent broadcasts because the best path selection using MBCF and node IDs information are already updated in the routing table for the same probability $P > 0$. The optimization is further extended towards an attenuation-based strategy once ProbaCvg completes or is interrupted during transmission for E_{LOW} or T_{HIGH}. The attenuation-based strategy adaptively takes over the transmission by considering the lowest attenuation level of neighbors. However, by default BothMinAtt requests prior attenuation values to each transmission, which is communication overhead. Therefore, the above-referred strategy used in this research is slightly modified where attenuation values in the routing table are updated from time to time by asking $Att.Request.Ask_{Advance}$ through control messages.

3) EXPLANATION AND EXAMPLE

The sink is a super-node from where the network tree usually grows. The sink node is always at the top and directly linked to a parent node. It results in elongated trees when more children and sub-children are added. Keeping in view above, this research proposes a distributive approach to create a dynamic network. The distributive approach allows to create multiple network points originating from more than one parent $P_a, P_b, P_c, \ldots, P_n$ linked to a single sink S_o. The sink node is assumed in the central position, preferably at waist height. The proposed protocol creates an optimized convergecast tree $C_T = C1 + C2 + C3$ where $C1$, $C2$, and $C3$ are independent convergecast trees. The possible convergecast trees are shown in Fig. 8(a), (b), and (c). Consider Fig. 8(a), which endorses the first possible node combination with a parent node P_a such that $C1 = P_a \to 2, 3$ has a total of $N = 3$ convergecast members. The second possible combination is $C1 = P_b \to 6, 7, 5$ has $N = 4$ convergecast members. $C1 = P_c \to 9, 10, 11$ has also $N = 4$ convergecast members. Here Node-11 is a new node that has requested to be a child member of either P_b or P_c. So, the corresponding set root node pair for $C1$ (P_a) is $RNP = \{(s_o \to 1, 2), (s_o \to 1, 3)\}$ and the number of paths towards RNP is, NP(i) = 2; i = 1, 2 with hop count H = 2. The corresponding set root node pair for $C1(P_b)$ is $RNP = \{(s_o \to 4, 5), (s_o \to 4, 6), (s_o \to 4, 6, 7)\}$ and the number of paths towards RNP is, NP(i) = 3; i = 1, 2, 3 with a maximum hop count of H = 3. The corresponding root node pair set for $C1(P_c)$ is $RNP = \{(s_o \to 8, 9), (s_o \to 8, 10), (s_o \to 8, 10, 11)\}$ and the number of paths towards RNP is, NP(i) = 3; i = 1, 2, 3 with maximum hop count H = 3. Considering that all the nodes are reliable, having high calculated by MBCF. The path set (P) for $C1(P_a)$ towards sink is $P_1 = (S_o \to 1, 2, 3)$, for $C1(P_b)$ is $P_2 = (S_o \to 4, 5, .., 6, 7)$, and for $C1(P_c)$ is

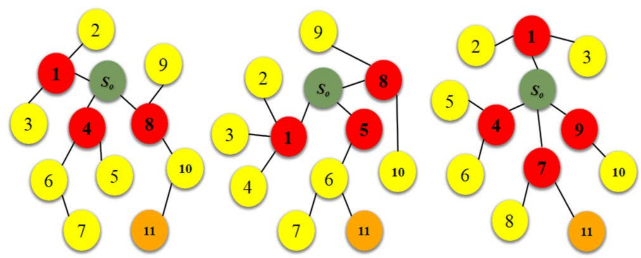

FIGURE 8. C_Tree_1 (C1), b. C_Tree_2 (C2), c. C_Tree_3 (C3). C1 is the first possible convergecast tree, with S_o as a sink and Node-ID 1, 4, 8 as the parent nodes P_a, P_b, and P_c. C2 is the second possible convergecast tree, with S_o as a sink and Node-ID 1, 5, 8 as the parent nodes P_a, P_b, and P_c. C3 is the third possible and preferred convergecast tree with the most parent-child distributions, with S_o as a sink and Node-ID 1, 4, 7, 9 as the parent nodes P_a, P_b, P_c, and P_d. Node-11 is a new candidate to join the network.

TABLE 7. Pseudocode of convergecast process.

Pseudocode – Convergecast

```
# Optimized Convergecast Tree
Repeat
Create Convergecast Tree G' = (V', E')
If H_a,b ≤ 2 && MBCF_MEAN == Highest
        Begin ProbaCvg
        If P > 0 && r < p
                Forward packet
        Else    Begin BothMinAtt
                Forward packet to the node with the
                lowest attenuation
End If All
Until the packet reach the sink node
```

$P_3 = (S_o \rightarrow 8, 9, .., 10, 11)$. However, among possible convergecast trees, Fig. 8(c) is a hot favorite because it has the highest parent-child distribution rate, as endorsed by the proposed protocol such that $\gamma_i 5 \leq 2$ as modeled in (15).

The convergecast tree $G' = (V', E')$ process begins at $o(1)$ where V is the number of nodes. The overall complexity depends on the initial broadcast in time $O(V)$. The complexity doubles $O(2V)$ when BothMinAtt takes over ProbaCvg for a backup route. The space complexity m proceeds in the same manner at $O(2m)$ for each node $o(m)$. Hence, the overall time and space complexities will be $O(V \times m)$.

A complete process flow diagram of the proposed protocol is given in Fig 9.

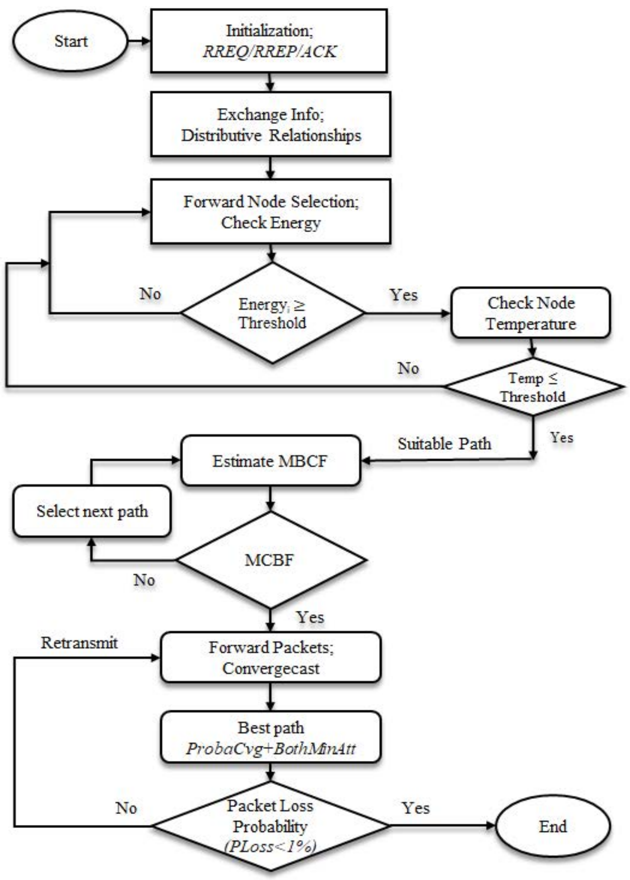

FIGURE 9. Process flow diagram of the proposed protocol.

IV. RESULTS AND DISCUSSION

The proposed protocol adopts an optimized convergecast strategy that collects data from child to root in an efficient manner and provides a backup route with reduced delay and increased throughput. It adopts multiple parent-child relationships to avoid a single root point failure. The recurrent broadcasts are reduced at initialization, parent-child polling, and convergecast strategy to lower communication and processing overheads, which also contributes to increased throughput and reduced E2E. In addition, the proposed protocol effectively preserves the thermal effect and improves energy efficiency.

Castalia, an Omnet++ framework [41] specially designed to simulate low-power embedded networks such as WSN and WBAN, is used in this research. Castalia is based on the IEEE 802.15.6 standard for testing protocols and distributed algorithms with realistic wireless channel and radio models. It has a highly parametric architecture that supports simulation of a wide range of platforms for realistic data, improved channel models, temporal variations, and mobility. Simulation parameters taken in the proposed protocol are listed in Table 8.

TABLE 8. Simulation parameter in castalia

Name of Parameter	Description
Number of Nodes	10
Initial Energy	18720 Joule
Radio	914 MHz
Bandwidth	1Mb
Distance	35 inches (< 1 meter)
Packet Size (Byte)	100 Min., 1000 Max.
Number of Packets	100 Min., 1000 Max.
Standard	IEEE 802.15.6
Packet Rate	Min 14, Max 30
Packet Interval Time	0.5 sec
Packet Retries	3
Run Time	2000 sec
No. of Transmission	50
No. of Simulations	50
Radio.TxOutputPower	-15dBm
Mobility	None
Duty cycle	100%

A. ASSUMPTIONS AND THRESHOLDS

1) The maximum transmission distance $T_{DISTANCE}$ is kept small (<1m) between each node with the same initial energy levels.
2) Each node has a static transmission power and range.
3) A fixed-sized packet is transmitted by every sensor, and each node transmits data at its time slot.

B. SINK NODE POSITION

The proposed protocol prioritizes sink placement so that it is easily accessible to other nodes with a high packet delivery ratio (PDR). Positions such as waist, head, and ankle are assumed through different hop counts because it is difficult to simulate sensor positions. The proposed protocol, as previously stated, endorses a distributed relationship with a maximum of two hops. This is because the network is initially allowed to grow in an unrestricted manner. A ten node network is set up for simulation testing, and four groups are formed to validate the waist, head, and ankle positions. These groups are separated by an equal distance with different hop counts, such as a single hop for the first group, two hops for the second group, three hops for the third group, and four hops for the final group. The simulation results show a low PDR from groups three and four for various numbers of transmissions, leading us to a restriction of the hop count

TABLE 9. Details of sensors, assigned threshold, and frequency.

Sensor	Threshold	Frequency
Electrocardiogram (ECG)	60 to 100 (diastolic)	Daily
Temperature	36.5 to 37.5 °C (97.7 to 99.5 °F)	Six hours
Blood glucose (BG)	80 to 130 mg/dL	Eight hours
Blood pressure (BP)	120/80 mmHg	Three hours
Pulse oximeter (SpO2)	90 to 100% O_2 70 to 100 bpm	Weekly
Respiration, Asthma, Pulmonary, Cough, Allergic rhinitis, Nose	12 to 16 breaths per minute (bpm)	Need-based

to a bare minimum such as two hops. The head and ankle positions do not satisfy the two-hop restriction because of the internal distance between the nodes, whereas the waist is an ideal position where each node can easily reach him. The first five nodes are at a single-hop distance from the sink, while the rest are at a two-hop distance.

PDR is the ratio of received packets by the receiver $TotPac_{Rec}$ in comparison to the total sent packets $TotPac_{Sent}$ as depicted in (32).

$$PDR = \frac{TotPac_{Rec}}{TotPac_{Sent}} \tag{32}$$

PDR is directly proportional to the distance between the source and sink node [42]. The initial transmission begins with hundred packets and gradually increases over the course of ten communication cycles. Each cycle adds a hundred packets to conclude the tenth transmission of one thousand packets as shown in Fig 10.

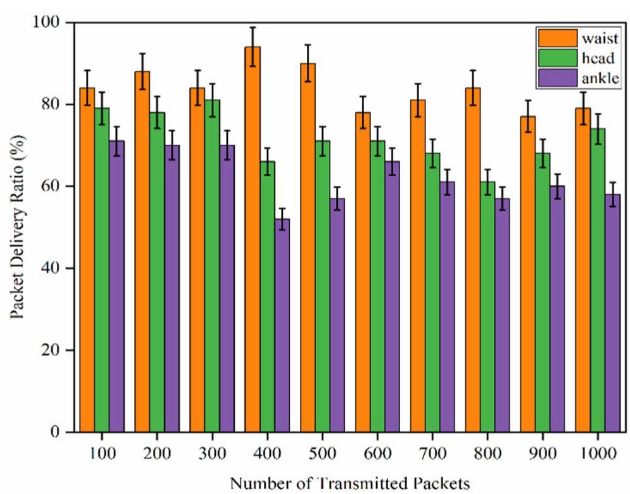

FIGURE 10. PDR – Position of sink node for an equal number of transmissions showing waist position has high PDR with ± 5% error.

The results in Fig. 10 show that received packets at the sink node have low PDR variation during the initial transmission cycle. The variation grows, particularly from nodes within two hops of each other. Also, PDR degradation is observed as simultaneous transmissions in multi-node contributions increase. It is worth noting that in WBAN, biosensors are installed in known locations for a dedicated purpose, such as the ECG, which is a regular transmitter, whereas oxygen saturation is not. The proposed protocol fully utilizes periodic and non-periodic activity-based transmissions to improve PDR. The results show an average PDR of 88% at one hop distance and an average of 79.8% at a two-hop distance. The number of packets and transmissions does not affect PDR, however, it gradually degrades to 68% in concurrent multi-node cooperation. The simulation outcomes demonstrate that the position of the sink node is an absolute requirement for an efficient network and successful data delivery.

C. TEMPERATURE RISE

The common thermal impacts on sensor nodes are internal computation, transmissions, and activity duration. The proposed model calculates total thermal variation ΔT_{TOTAL} as a difference between the current thermal value $\Delta T_{CURRENT}$ and its initial thermal value $\Delta T_{INITIAL}$ of sensor node. A maximum operating temperature of a standard node is 140°F (60°C) and normal body temperature ranges from 97°F (36.1°C) to 100.3°F (37.95°C) and below skin harmful value is 111.2°F (44°C) [43]. Existing thermal-aware protocols make decisions based on temperature values, whereas cross-layer protocols are mainly not thermal-aware. The simulation tests are performed on ten nodes without including any relay nodes. The calculated thermal variations are shown in Fig.11.

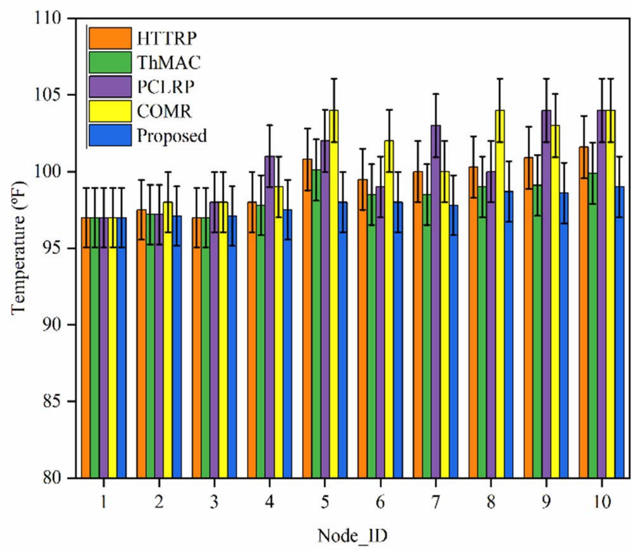

FIGURE 11. Comparison of the proposed protocol with thermal-aware and cross-layer protocols for temperature rise with ± 1% error.

The results show that the proposed protocol is thermally aware by keeping thermal variations within the bounds in comparison to COMR, PCLRP, ThMAC, and HTTRP. Fig.11 depicts nearly identical thermal variations in Nodes 1, 2, and 3. These nodes are non-periodic, non-forwarding, and in two-hop distance from the sink node. However, Node-4 to 10 are periodic nodes especially Node-5 (ECG), Node-9 (Glucose), and Node-10 (BP), which are involved in critical activities that contribute to the rapid thermal rise. These nodes require a more controlled environment than other non-periodic nodes. The network load is distributed so that the referred nodes can perform in constant time gaps, and once an activity is completed, it forces them to sleep quickly. The proposed protocol keeps the temperature within limits due to distributive parent-child relationships, which reduces communication overhead. Moreover, convergecast provides an alternate route by preventing these nodes from frequently forwarding packets from other nodes, which also reduces temperature rise.

D. THROUGHPUT

The actual volume of packets that successfully arrive at the sink node in a defined time is referred to as throughput. Throughput performance is critical in WBAN because it assumes a successful communication link between nodes, making it an important parameter to determine network performance [44]. The results are evaluated by considering periodic P_N communication. The parametric contributions are closely examined to understand their impact on throughput behavior. The simulation results show a high throughput in comparison to COMR, PCLRP, ThMAC, and HTTRP protocols. The proposed protocol's results are validated by analyzing the number of participating sensors, packet transmission, and total throughput in unit kilobits per second (Kbps). Initially, in the first round r, a hundred packets are transmitted at a 0.5-second interval for a total of fifty transmissions. The simulation parameters such as runtime and number of packets are extended to test individual round performance for maximum successful delivery rates. Each round adds a hundred packets, up to a total of a thousand packets in the final round. The proposed protocol's performance in comparison to other protocols is shown in Fig. 12.

Fig. 12 shows a close comparison of proposed protocol performance in each round, with an improvement ranging from 8% to 13.75% in the final rounds. Overheads such as redundant broadcasts, congestion, and hop counts are reduced in order to improve throughput, especially during enforcement of the ProbaCvg convergecast strategy. According to the simulation results, the throughput increases when the number of nodes and transmission packets increases. The growth rate of the cross-layer COMR and PCLRP protocols is somewhat closer to the proposed protocol growth rate due to their low transmission cycle and non-thermal awareness. However, the proposed protocol shows an improved performance from round 8^{th} onwards ($r \geq 8$). Fig.12 shows that the proposed protocol outperforms other protocols in all rounds due to its distributive approach and optimized convergecast strategy. It efficiently reduces concurrent transmissions from other nodes that generate traffic, and network congestion prevents packets from being forwarded adaptively. The proposed protocol considers packet priority and transmission delay into

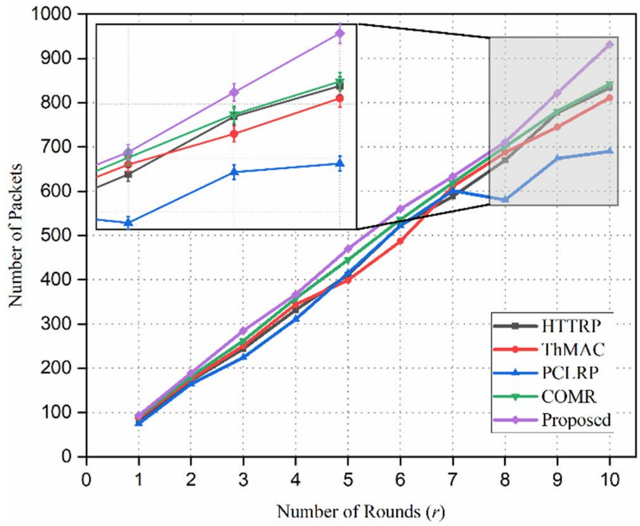

FIGURE 12. Throughput comparison of the proposed protocol with COMR, PCLRP, ThMAC, and HTTRP with ± 1% error.

consideration, which is evident in the final rounds, such as 8% in the ninth round and 13.75% in the tenth round.

E. E2E DELAY

Routing protocols encounter complications such as multiple route requests, energy levels, congestions, and high temperatures when attempting to find the best route. E2E delays are eventually caused by such complications involving multiple devices in short transmission gaps. The above-mentioned conditions are kept in mind throughout the simulation by ensuring stable links and limiting the total number of packets to one thousand. The simulation time, the number of packets and the number of transmissions are all increased to see if any further improvements can be made. The WBAN architecture supports emergency, normal, and on-demand transmissions. The proposed protocol focuses on normal transmission because it is a periodic transmission that occurs at regular intervals. Initially, a hundred-second transmission cycle is used, and the entire transmission is completed for a total of two thousand seconds of simulation for fifty tests, as shown in Fig. 13.

The results in Fig. 13 show that delays are high during the initial deployment phase due to the flooding of control messages in the initialization process. Other factors that contribute to network delay include routing mechanisms, large queues, link reliability, and node response. The proposed protocol efficiently considers the stated factors once the network converges. The delay gradually decreases in the middle rounds with an average improvement of 19.14% in an average 100-second interval. Delays are most likely being reduced as a result of distributive parent-child relationships and low hop counts. The use of an alternate route adds a small amount of delay, which is negligible in the context of WBAN because delay usually improves throughput [45]. Using an alternate route, which is provided by convergecast, is less expensive in terms of delay than re-polling for the parent node.

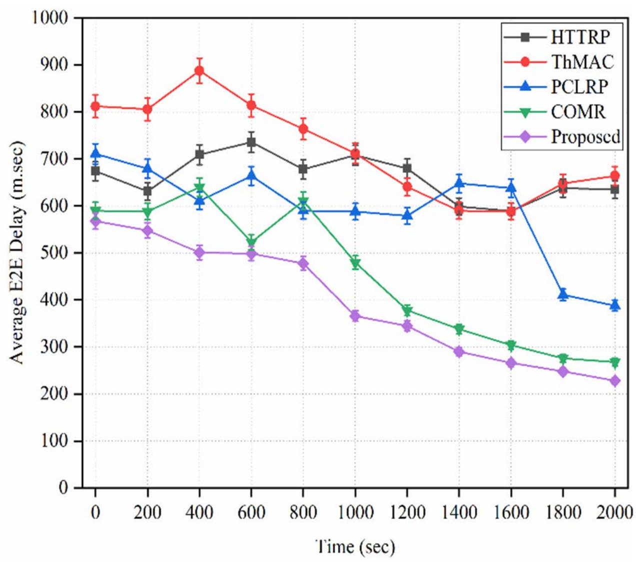

FIGURE 13. E2E comparison of the proposed protocol with COMR, PCLRP, ThMAC, and HTTRP with ± 3% error.

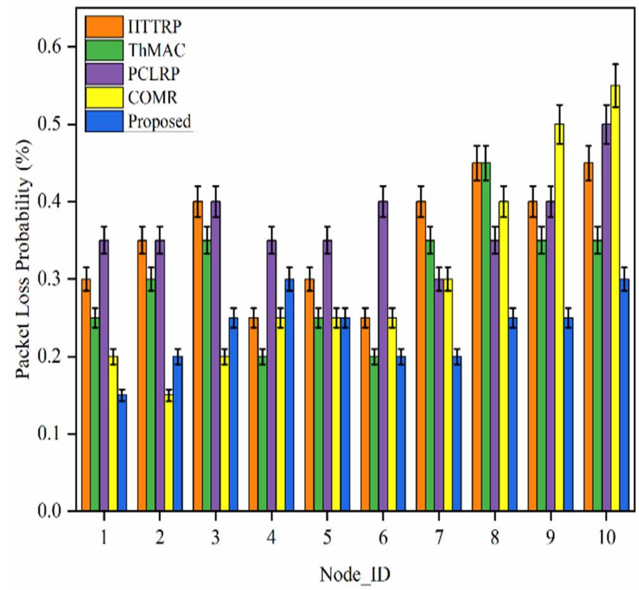

FIGURE 14. Packet loss comparison of the proposed protocol with COMR, PCLRP, ThMAC, and HTTRP with ± 5% error.

F. PACKET LOSS PROBABILITY

The packet loss probability is a useful parameter to ensure energy efficiency and accurate results, especially during link outages. The proposed protocol guarantees stable links to provide a conducive environment for packet flow to reach the sink in its original form. Once the network has successfully converged, the error rate of each transmission is verified at the sink node via calculating the number of packets transmitted from the source and receiving the same number at the sink node. Any deviation in the sequence or number of packets in a single transmission cycle results in a retransmission request from the sink node. However, retransmission consumes additional resources, and frequent retransmission is not an efficient approach. Therefore, the proposed protocol with an optimal, distributive, and low hop count network reduces the chances of retransmission. Packet loss usually happens due to congestion, poor signals, natural/man-made interference, system noise, and hardware/software failure [46]. In this research, a total of ten nodes are validated for a maximum of one thousand packets, as shown in Fig. 14.

All the deployed nodes (near and far) have an optimal delivery rate of packets due to the distributed approach, however, it increases the delay. The nodes far from the sink (distance '2-hops') have less than 0.3% probability, indicating that an increase in the number of hops reduces performance. The results show that stable links provide a conducive network environment for successful packet delivery. Increasing the transmission load and time slots increases packet loss and delay. It causes packets to take longer than usual time to reach their destination. Additionally, the packet loss probability increases to 0.9% during route repairs and parent-child polling. However, it can be controlled by using stable/adaptable links, increasing the number of packets, and reducing time slots. The proposed protocol uses stable and optimal paths to route data in its original form. The sink node obtains accurate data in various conditions, such as route failures, parent-child selections, and alternate routes by showing the low packet loss probability.

G. DISCUSSION

The proposed protocol is optimized and distributive in nature, focusing on optimum route selection and reduced broadcasts to improve throughput, reduce packet delay and energy consumption, and provides reliable communication in normal and emergency cases. It provides stable convergence by reducing unnecessary broadcasts and handshakes, thereby reducing communication and processing overheads. The distributive approach in a maximum of two hops avoids a single root point dependency. Hence, there are no pre-defined nodes that can act as a single parent or child. The optimal route updates upon the start of any priority transmission, allowing new metrics to be recorded and assisting all packets in choosing the best route to encourage adaptability.

The simulation results show the performance of the proposed theoretical analysis in Castalia for a network of ten sensors and one sink node with fixed positions. Castalia adheres to the IEEE 802.15.6 standard that deduces stationary nodes in single unit transmission and range. MAC layer broadcasts and acknowledgments are used where necessary and avoided where possible. Besides basic simulation parameters, the simulation transmissions are extended to one thousand transmissions to determine the best sink node position, thermal rise, throughput, E2E delay, and packet loss probability. However, there is no major variation between results observed except for throughput. The proposed protocol's performance is compared with COMR, PCLRP, ThMAC, and HTTRP protocols. The comparative analysis in Fig.11, 12, 13, and 14

TABLE 10. Operational comparison of the proposed protocol with other routing protocols.

Parameter	[48]	[49]	[50]	Proposed
Theme	Directed Diffusion	Block Chain	Man-in-Middle attack	Convergecast
Workflow	Random, Mesh topology	Not mentioned	Privacy-preserving, hierarchical	Steady, regular
Data distribution	Data-centric	Data-driven	Data-aggregation	Data-centric, data-driven
Method	Query-based	Event-based	Event-based	Query and Event-based
Propagation	Interest-based	Transaction-based	Cluster-based	Distributive (max. 2-hops)
Data Transmission	Broadcasts	Broadcasts	Not mentioned	Broadcast, Multicast, Unicast
Mode	One to many	One to one	Many to one	Many to one
Cross Platform	None	WBAN, Blockchain	Cross-layer	Cross-layer, Thermal-aware
Path selection	Path enhancement, hop count	Energy, Heat	Energy, Distance	Energy, Heat, Pathloss, Linkloss, Bandwidth, Hop count
Data Priority	None	None	None	Emergency, On-demand, Normal

shows improvement in network throughput, decrease E2E delay, and decrease packet loss probability while keeping the temperature of sensor nodes within the limit. The optimization adjustment with respect to broadcasts with a novel convergecast strategy has significantly reduced packet drops, packet processing delay, and increased packet flow, which results in improved throughput, and reduced E2E delay. The proposed protocol efficiently handles the traffic loads with an average minimal delay of 19.14%, and improved throughput achieving 8% in the ninth round and 13.75% in the tenth round. The packet loss probability is also kept under 0.3% for all simulation rounds. To double-check and validate correctness, the number of simulations and the number of run-times are increased to hundred rounds for ten thousand seconds, resetting the statistics after one thousand to eliminate any tradeoffs. The long simulation improves results from 10% to 20%, with an 83.7% delivery rate. Although the proposed protocol increases transmission delay during the convergence process, it manages to keep it under 0.1sec. Due to the distributive novel convergecast strategy, it is observed that (i) simultaneous transmission increases packet loss, and has a higher thermal effect with reduced throughput; (ii) larger packets and longer delays reduce packet loss and minimize the thermal effect.

The convergecast uses ProbaCvg by default, and if a parameter threshold is exceeded, another semi-stable route under BothMinAtt is enforced with no additional delay. The execution is also affected by how many backward hops are covered to adjust the next hop selection values. It loses some packets during the process because the convergecast collects data in many-to-one patterns and employs two strategies. The route-fixing process has an average permanent failure rate of 2–5% [47].

Moreover, the proposed convergecast protocol is compared with other routing protocols such as [48], [49], and [50]. The performance of the proposed protocol is validated against a variety of parameters keeping in view efficient communication in the WBAN environment. A detailed comparison is given below in Table 10.

The proposed protocol results are not validated for node mobility and wireless channel temporal variation that happens normally due to rapidly changing environments. Different body postures are frequent which also affects connectivity in WBAN. To improve connectivity, the power level of the radio needs to be increased which also itself is a limitation in respect of energy consumption and heat production.

V. CONCLUSION

WBAN is a resource-constraint network requiring an optimized, distributive, and adaptive routing protocol. The proposed routing protocol efficiently achieves rapid convergence by reducing communication and processing overheads. It also avoids a single root point failure through distributive parent-child relationships. Moreover, the proposed protocol is thermally aware. The routing table periodically updates critical parameters for the next best hop selection via MBCF. If a node has low energy or hotspot, it will stop forwarding data but continue to send emergency data, if necessary. The data is collected in a many-to-one pattern using a novel hybrid convergecast strategy, which improves data flow and adaptability if an unstable route is discovered. The successful transmission is checked for packet loss probability to ensure data integrity and restore any local loss. The simulation results reveal that the proposed protocol is optimized, distributive, and thermally aware compared to the state-of-the-art cross-layer and thermal-aware protocols.

In the future, we intend to validate other convergecast mechanisms, such as multipath-based, attenuation-based, and dynamic path-based testing. A complete framework will be developed by incorporating previous work. We intend to generate local healthcare datasets through an embedded sensor technology using the proposed protocol. The data will be forecast through edge computing and aggregated for medical professionals to make onsite decisions.

ACKNOWLEDGMENT

The authors would like to thank the support of Prince Sultan University for paying the article processing charges (APC) of this manuscript.

REFERENCES

[1] V. Kale, C. Katke, S. Dayane, and P. Thakar, "Challenges of introducing lean six sigma, IoT in industry 4.0, and supply chain management: A review," in *Intelligent Manufacturing and Energy Sustainability*, vol. 265. Singapore: Springer, 2022, pp. 303–315.
[2] S. Liu and Y. Xu, "Exploring innovative development strategies for safety education in the context of big data and the Internet of Things," *Wireless Commun. Mobile Comput.*, vol. 2022, pp. 1–8, Mar. 2022.
[3] O. Djumanazarov, A. Vaananen, K. Haataja, and P. Toivanen, "An overview of IoT-based architecture model for smart home systems," in *Intelligent Systems Design and Applications*, vol. 418. Switzerland: Springer, Mar. 2022, pp. 696–706.
[4] C. Chen, J. Jiang, Y. Zhou, N. Lv, X. Liang, and S. Wan, "An edge intelligence empowered flooding process prediction using Internet of Things in smart city," *J. Parallel Distrib. Comput.*, vol. 165, pp. 66–78, Jul. 2022.

[5] V. K. Quy, V. N. Hau, D. V. Anh, N. M. Quy, N. T. Ban, S. Lanza, G. Randazzo, and A. Muzirafuti, "IoT-enabled smart agriculture: Architecture, applications, and challenges," *Appl. Sci.*, vol. 12, no. 7, pp. 1–19, Mar. 2022.

[6] V. Bhardwaj, R. Joshi, and A. M. Gaur, "IoT-based smart health monitoring system for COVID-19," *Social Netw. Comput. Sci.*, vol. 3, no. 2, pp. 1–11, Jan. 2022.

[7] M. M. Nasralla, "Sustainable virtual reality patient rehabilitation systems with IoT sensors using virtual smart cities," *Sustainablity*, vol. 13, no. 9, pp. 1–15, Apr. 2021.

[8] Y. A. Qadri, A. Nauman, Y. B. Zikria, A. V. Vasilakos, and S. W. Kim, "The future of healthcare Internet of Things: A survey of emerging technologies," *IEEE Commun. Surveys Tuts.*, vol. 22, no. 2, pp. 1121–1167, Feb. 2020.

[9] F. Ullah, A. H. Abdullah, O. Kaiwartya, S. Kumar, and M. M. Arshad, "Medium access control (MAC) for wireless body area network (WBAN): Superframe structure, multiple access technique, taxonomy, and challenges," *Hum.-centric Comput. Inf. Sci.*, vol. 7, no. 1, pp. 1–39, Dec. 2017.

[10] V. Mekathoti and B. Nithya, "A survey on congestion control algorithms of wireless body area network," in *Advances in Computing and Network Communications*. Singapore: Springer, Apr. 2021, pp. 373–387.

[11] N. Ahmad, B. Shahzad, M. Arif, D. Izdrui, I. Ungurean, and O. Geman, "An energy-efficient framework for WBAN in health care domain," *J. Sensors*, vol. 2022, pp. 1–11, Feb. 2022.

[12] Z. Huang, Y. Cong, Z. Ling, Z. Mao, and F. Hu, "Optimal dynamic resource allocation for multi-point communication in WBAN," *IEEE Access*, vol. 8, pp. 114153–114161, 2020.

[13] X. Chen, Y. Xu, and A. Liu, "Cross layer design for optimizing transmission reliability, energy efficiency, and lifetime in body sensor networks," *Sensors*, vol. 17, no. 4, pp. 1–32, Apr. 2017.

[14] H. Zhang, F. Safaei, and L. C. Tran, "Joint transmission power control and relay cooperation for WBAN systems," *Sensors*, vol. 18, no. 12, pp. 1–26, Dec. 2018.

[15] K. G. Mkongwa, Q. Liu, and C. Zhang, "Link reliability and performance optimization in wireless body area networks," *IEEE Access*, vol. 7, pp. 155392–155404, 2019.

[16] P. Wikanta, A. Triwinarko, I. Dayoub, and E. H. Dogheche, "A cross layer protocol PHY/MAC for body pathloss in IEEE 802.11ah IoT networks," in *Proc. IEEE SENSORS*, Rotterdam, The Netherlands, Oct. 2020, pp. 1–4.

[17] H. B. Elhadj, J. Elias, L. Chaari, and L. Kamoun, "A priority based cross layer routing protocol for healthcare applications," *Ad Hoc Netw.*, vol. 42, pp. 1–18, May 2016.

[18] U. F. Abbasi, N. Haider, A. Awang, and K. S. Khan, "Cross-layer MAC/routing protocol for reliable communication in Internet of Health Things," *IEEE Open J. Commun. Soc.*, vol. 2, pp. 199–216, 2021.

[19] F. Ullah, M. Z. Khan, G. Mehmood, M. S. Qureshi, and M. Fayaz, "Energy efficiency and reliability considerations in wireless body area networks: A survey," *Comput. Math. Methods Med.*, vol. 2022, pp. 1–15, Jan. 2022.

[20] N. Javaid, Z. Abbas, M. S. Fareed, Z. A. Khan, and N. Alrajeh, "M-ATTEMPT: A new energy-efficient routing protocol for wireless body area sensor networks," *Proc. Comput. Sci.*, vol. 19, pp. 224–231, Jan. 2013.

[21] A. R. Bhangwar, P. Kumar, A. Ahmed, and M. I. Channa, "Trust and thermal aware routing protocol (TTRP) for wireless body area networks," *Wireless Pers. Commun.*, vol. 97, no. 1, pp. 349–364, Nov. 2017.

[22] M. Javed, G. Ahmed, D. Mahmood, M. Raza, K. Ali, and M. U. Rehman, "TAEO-A thermal aware & energy optimized routing protocol for wireless body area networks," *Sensors*, vol. 19, no. 15, pp. 1–14, Aug. 2019.

[23] S. Bouldjadj and Z. Aliouat, "High throughput and thermal aware routing protocol (HTTRP) for wireless body area networks," *Ingénierie des Systèmes Inf.*, vol. 25, no. 1, pp. 41–48, Feb. 2020.

[24] M. M. Monowar and M. O. Alassafi, "On the design of thermal-aware duty-cycle MAC protocol for IoT healthcare," *Sensors*, vol. 20, no. 5, pp. 1–20, Feb. 2020.

[25] E. Selem, M. Fatehy, and S. M. A. El-Kader, "MobTHE (mobile temperature heterogeneity energy) aware routing protocol for WBAN IoT health application," *IEEE Access*, vol. 9, pp. 18692–18705, 2021.

[26] Y. Shahzad, H. Javed, H. Farman, J. Ahmad, B. Jan, and A. A. Nassani, "Optimized predictive framework for healthcare through deep learning," *Comput., Mater. Continua*, vol. 67, no. 2, pp. 2463–2480, 2021.

[27] M. Adnan, F. Sallabi, K. Shuaib, and M. Abdul-Hafeez, "Performance enhancement of IEEE 802.15.6 using collision avoidance technique," *J. Sensor Actuator Netw.*, vol. 9, no. 33, pp. 1–21, Jul. 2020.

[28] Y. Shahzad, H. Javed, H. Farman, J. Ahmad, B. Jan, and M. Zubair, "Internet of Energy: Opportunities, applications, architectures and challenges in smart industries," *Comput. Electr. Eng.*, vol. 86, pp. 1–20, Sep. 2020.

[29] A. Alkhayyat, S. F. Jawad, and S. B. Sadkhan, "Cooperative communication based: Efficient power allocation for wireless body area networks," in *Proc. 1st AL-Noor Int. Conf. Sci. Technol. (NICST)*, Sulimanyiah, Iraq, Oct. 2019, pp. 106–111.

[30] M. Kortas, O. Habachi, A. Bouallegue, V. Meghdadi, T. Ezzedine, and J. P. Cances, "The energy-aware matrix completion-based data gathering scheme for wireless sensor networks," *IEEE Access*, vol. 8, pp. 30772–30788, 2020.

[31] Y. B. Chaouche, M. Nedil, I. B. Mabrouk, and O. M. Ramahi, "A wearable circularly polarized antenna backed by AMC reflector for WBAN communications," *IEEE Access*, vol. 10, pp. 12838–12852, 2022.

[32] O. Ahmed, F. Ren, A. Hawbani, and Y. Al-Sharabi, "Energy optimized congestion control-based temperature aware routing algorithm for software defined wireless body area networks," *IEEE Access*, vol. 8, pp. 41085–41099, 2020.

[33] Y. Qu, G. Zheng, H. Wu, B. Ji, and H. Ma, "An energy-efficient routing protocol for reliable data transmission in wireless body area networks," *Sensors*, vol. 19, no. 19, pp. 1–15, Sep. 2019.

[34] M. Waheed, R. Ahmad, W. Ahmed, M. Drieberg, and M. M. Alam, "Towards efficient wireless body area network using two-way relay cooperation," *Sensors*, vol. 18, pp. 1–23, Feb. 2018.

[35] D. A. Hammood, H. A Rahim, R. B. Ahmad, A. Alkhayyat, M. E. M. Salleh, M. Abdulmalek, M. Jusoh, and Q. H. Abbasi, "Enhancement of the duty cycle cooperative medium access control for wireless body area networks," *IEEE Access*, vol. 7, pp. 3348–3359, 2019.

[36] A. Alkhayyat and M. S. Mahmoud, "Hybrid network coding and cooperative communication in WBAN," in *Proc. 2nd Int. Conf. Eng. Technol. its Appl. (IICETA)*, Al-Najef, Iraq, Aug. 2019, pp. 79–82.

[37] H. Al-Mishmish, A. Alkhayyat, H. A. Rahim, D. A. Hammood, R. B. Ahmad, and Q. H. Abbasi, "Critical data-based incremental cooperative communication for wireless body area network," *Sensors*, vol. 18, pp. 1–19, Oct. 2018.

[38] G. Bu and M. Potop-Butucaru, "BAN-GZKP: Optimal zero knowledge proof based scheme for wireless body area networks," *Ad Hoc Netw.*, vol. 77, pp. 28–41, Aug. 2018.

[39] N. Choudhury, M. M. Nasralla, P. Gupta, and I. Ur Rehman, "Centralized graph based TSCH scheduling for IoT network applications," in *Proc. IEEE Int. Conf. Parallel Distrib. Process. Appl., Big Data Cloud Comput., Sustain. Comput. Commun., Social Comput. Netw. (ISPA/BDCloud/SocialCom/SustainCom)*, New York, NY, USA, Sep. 2021, pp. 1639–1644.

[40] N. Choudhury and M. M. Nasralla, "A proposed resource-aware time-constrained scheduling mechanism for DSME based IoV networks," in *Proc. IEEE 94th Veh. Technol. Conf. (VTC-Fall)*, Norman, OK, USA, Sep. 2021, pp. 1–7.

[41] M. Kaur, "Performance and scalability evaluation of the wireless body area network using Castalia simulator," *Turkish J. Comput. Math. Educ.*, vol. 12, no. 2, pp. 543–554, Apr. 2021.

[42] K. Karunanithy and B. Velusamy, "Edge device based efficient data collection in smart health monitoring system using wireless body area network," *Biomed. Signal Process. Control*, vol. 72, pp. 1–14, Feb. 2022.

[43] H. Arslan, M. Keskin, H. Zengin, and G. Zengin, "Glucose biosensing at carbon paste electrodes containing polyaniline-silicon dioxide composite," *Int. J. Electrochem. Sci.*, vol. 7, no. 10, pp. 10205–10214, Oct. 2012.

[44] A. Alkhayyat and N. A. Habeeb, "A cooperative MAC aware network coding toward improving throughput wireless body area network," in *Proc. 2nd Sci. Conf. Comput. Sci. (SCCS)*, Baghdad, Iraq, Mar. 2019, pp. 182–187.

[45] R. Saha and S. Biswas, "Analytical study on data transmission in WBAN with user mobility support," in *Proc. Int. Conf. Wireless Commun., Signal Process. Netw. (WiSPNET)*, Chennai, India, Mar. 2018, pp. 1–5.

[46] L. Rajendran and P. Vetrivelan, "Wireless body area network (WBAN)-based telemedicine for emergency care," *Sensors*, vol. 20, no. 7, pp. 1–18, Apr. 2020.

[47] F. Araujo, A. Gomes, and R. P. Rocha, "Towards optimal convergecast in wireless ad hoc networks," *Ad Hoc Netw.*, vol. 107, pp. 1–14, Oct. 2020.

[48] J. Mu, X. Yi, X. Liu, and L. Han, "An efficient and reliable directed diffusion routing protocol in wireless body area networks," *IEEE Access*, vol. 7, pp. 58883–58892, 2019.

[49] Z. Shahbazi and Y.-C. Byun, "Towards a secure thermal-energy aware routing protocol in wireless body area network based on blockchain technology," *Sensors*, vol. 20, no. 12, pp. 1–26, Jun. 2020.

[50] A. Kore and S. Patil, "IC-MADS: IoT enabled cross layer man-in-middle attack detection system for smart healthcare application," *Wireless Pers. Commun.*, vol. 113, no. 2, pp. 727–746, Apr. 2020.

YASIR SHAHZAD received the M.S. degree in computer science from the Department of Computer Science, University of Peshawar, Pakistan, in 2017. He is currently pursuing the Ph.D. degree with the Department of Computer Science. His research interests include the IoT, IoHT, IoE, deep learning, and wireless sensor networks.

HUMA JAVED received the Ph.D. degree in wireless sensor networks from Liverpool John Moores University, U.K., in 2007. Currently, she is working as an Assistant Professor with the Department of Computer Science, University of Peshawar, Pakistan. Her research interests include middleware for wireless sensor networks, smart health, ubiquitous, and pervasive computing.

HALEEM FARMAN received the M.S. degree from International Islamic University Islamabad, Pakistan, in 2008, and the Ph.D. degree from the University of Peshawar, Pakistan, in 2018. He is currently working as a Lecturer at the Department of Computer Science, Islamia College University Peshawar, Pakistan. His research interests include wireless sensor networks, the IoT, deep learning, and QoS issues in wireless networks.

ZAHID KHAN (Senior Member, IEEE) received the master's degree in computer science from the University of Sophia Antipolis, Nice, France, in 2015, and the Ph.D. degree in information and communication engineering from Southwest Jiaotong University, Chengdu, China, in 2019. He has completed a two years postdoctoral research with the Robotics IoT Laboratory, Prince Sultan University, Riyadh, Saudi Arabia, from 2019 to 2021, where he is currently a Researcher and a Faculty Member. He has published more than 25 research articles in leading journals and conference proceedings, including IEEE Transactions and Flagship conferences. His current research interests include IoT-based intelligent transportation, cluster-based routing schemes for VANETs, link reliability, and connectivity of VANETs.

MOUSTAFA M. NASRALLA (Senior Member, IEEE) received the B.Sc. degree (Hons.) in electrical engineering from Hashemite University, Jordan, in 2010, the M.Sc. degree in networking and data communications from Kingston University, London, U.K., in 2011, and the Ph.D. degree from the Faculty of Science, Engineering and Computing (SEC), Kingston University. He is currently an Associate Professor with the Department of Communications and Networks Engineering, Prince Sultan University (PSU), Riyadh, Saudi Arabia. He has published over 40 articles in high impact factor journals and reputable conferences. His research interests include the latest generation of wireless communication systems (e.g., 6G, 5G, LTE-A, and LTE wireless networks), wireless sensor networks, network security, the Internet of Things (IoT), machine learning, radio resource allocation, telemedicine and video compression, and multimedia communications. He is a fellow of the Higher Education Academy (FHEA). He is currently an Active Member of the Smart Systems Engineering Laboratory, PSU. He was a member of the Wireless Multimedia and Networking (WMN) Research Group, Kingston University. He served as an Active Reviewer and received several distinguished reviewer awards from several reputable journals, such as IEEE Transactions on Wireless Communications, IEEE Transactions on Multimedia, IEEE Transactions on Vehicular Technology, *Wireless Communications* (Elsevier), and *Computer Network* (Elsevier). He has solid research contributions in the area of networks and data communications which are proven with publications in reputable journals with ISI Thomson JCR. He has won several national and international funded projects, such as U.K. Home Office, EU FP7 CONCERTO, and 5G-enabled Smart City Development in Saudi Arabia. Currently, he is serving as a Guest Editor for *Alexandria Engineering Journal* (Elsevier), *International Journal of Distributed Sensor Networks* (SAGE), *Journal of Communications and Networks* (Frontiers) and an Organizer of the International Conference on Sustainability: Developments and Innovations, and the 5G-Enabled Smart Cities workshop in the 7th IEEE International Conference on Smart Cities. Moreover, he is a Senior Member of IEEE Young Professionals, IEEE ComSoc, and the Association of Computing Machinery (ACM).

ANIS KOUBAA is currently a Professor in computer science and the Leader of the Robotics and Internet of Things Research Laboratory, Prince Sultan University. He is also a Senior Researcher with CISTER and ISEP-IPP, Porto, Portugal, and a Research and Development Consultant with Gaitech Robotics, China. His current research interests include providing solutions toward the integration of robots and drones into the Internet of Things (IoT) and clouds, in the context of cloud robotics, robot operating systems (ROSs), robotic software engineering, wireless communication for the IoT, real-time communication, safety and security for cloud robotics, intelligent algorithm's design for mobile robots, and multi-robot task allocation. He is also a Senior Fellow of the Higher Education Academy (HEA), U.K. He has been the Chair of the ACM Chapter in Saudi Arabia, since 2014.